



# Practical application of Open Loop Onset Point Criterion to predict actuator rate saturation PIO in fly-by-wire aircraft

Juliano A. B. Gripp<sup>1</sup>, Marco A. G. Moreira<sup>2</sup>, Luís G. Trabasso<sup>3</sup>, and Cleverson M. P. Marinho<sup>4</sup>

<sup>1,2,4</sup> EMBRAER. Rod. Pres. Dutra, km 134, São José dos Campos, SP, 12247-820, Brazil

<sup>3</sup> ISI – Instituto SENAI de Inovação. R. Arno Waldemar Döhler, 308, Joinville, SC, 89218-153, Brazil

*Abstract: Actuator rate saturation has been a contributing factor for Pilot-Induced Oscillations (PIO) experienced on some aircraft incidents, indicating potential design problems of flight control laws. Some criteria to predict this kind of phenomenon during design has been proposed in last decades, such as the Open Loop Onset Point (OLOP) criterion. In order to explore the capacities of prediction and limitations of OLOP criterion applied to the design of representative flight control laws for a transport aircraft in full flight envelope, two methods of control laws to regulate roll rate and sideslip (“p-beta”) were evaluated. As first method, consider a dead zone for roll spoilers, such that roll spoilers deflect only after certain deflection of ailerons. As second method, consider that ailerons and roll spoilers work together whenever required. OLOP criterion was applied in both methods with maneuvers varying pilot gain, frequency, and amplitude. These combinations were compared in practical offline simulations. Results show that OLOP criterion can be adopted as a first filter to identify potential PIO scenarios, although it presents difficulties for setup. Benefits and limitations of OLOP application are highlighted.*

**Keywords: Nonlinear dynamics, Rate saturation, Open Loop Onset Point, Fly-by-wire Aircraft, Control Law**

## INTRODUCTION

Pilot-Induced Oscillation (PIO) problem has been present in aviation throughout the history of manned flight. PIOs have caused numerous accidents with results ranging from minor damage to total loss of the aircraft and pilot (Klyde et al., (1995)) and it is still a challenging topic of recent works such as Nguyen et al. (2021), Efremov et al. (2020). The military standard MIL-STD-1797B (USAF, 2006) defines PIO as “sustained or uncontrollable oscillations resulting from efforts of the pilot to control the aircraft”.

Some references such as GARTEUR (1999) present four categories to classify potentially severe PIOs: 1) Category I - Essentially Linear Pilot-Vehicle System Oscillations; 2) Category II - Quasi-Linear Pilot-Vehicle System Oscillations with Rate or Position Limiting (focus of this work); 3) Category III - Essentially Nonlinear Pilot-Vehicle System Oscillations with Transitions; 4) Category IV - Aeroservoelastic Coupling Oscillations.

The well-known theories for the analysis of Category I PIO focus on linear aircraft dynamics in the frequency domain, and the criteria documented for example in GARTEUR (1999) are largely accepted. However, the cited criteria are not enough to cover nonlinear effects in the frequency domain and predict Category II PIOs. Based on literature review, Open Loop Onset Point (OLOP) criterion from Duda (1997) is one of the most promising criteria to predict Category II PIOs, with a high degree of success for the cases evaluated, although some limitations have been found.

This paper highlights as contributions the challenges to apply the OLOP criterion to two versions of lateral-directional control laws for the whole flight envelope of a transport aircraft, assuming certain flap configuration. OLOP criterion was applied in both control laws with maneuvers varying pilot gain, frequency, and amplitude. Next sections provide an overview of aircraft for case study, control laws, and practical application of OLOP criterion.

## AIRCRAFT MODEL

To perform a representative flight control laws design, it is necessary to have detailed information about the aircraft. Considering the level of details from report such as NASA (1970), the airframe of the aircraft Boeing 747-100 (four-fanjet intercontinental transport aircraft) was adopted for this study. Figure 1(a) presents a schematic view of the aircraft, with emphasis in the control surfaces. This paper focuses attention on flap settings equal to 30 deg. Directional (yaw) control is obtained from two rudder segments (upper and lower rudder, assumed to move together). Lateral control system consists of inboard ailerons (High Speed Ailerons), outboard ailerons (Low Speed Ailerons) and roll spoilers. For simplicity, it is assumed that: inboard and outboard ailerons deflect together; only four most outboard spoiler panels (1, 2, 3, 4, 9, 10, 11, 12) were considered to actuate as roll spoilers. Moreover, it is assumed that the ailerons, rudders, and roll spoilers are driven by hydraulic actuators, with a full authority fly-by-wire control system.

A computational model for the aircraft (Figure 1(b)) was built using the software Simulink, described in Gripp et al. (2023), and it was validated comparing simulation results with data from report NASA (1970). The model inputs are

Throttle, deflection of Actuators and Mass Properties (Mass and Center of Gravity, CG). The main outputs are aircraft velocity ( $V$ ), Pressure Altitude (Alt), angular rates ( $p, q, r$ ), accelerations at CG ( $a_x, a_y, a_z$ ), Euler angles ( $\phi, \theta, \psi$ ) and aerodynamic angles ( $\alpha, \beta, \gamma$ ).

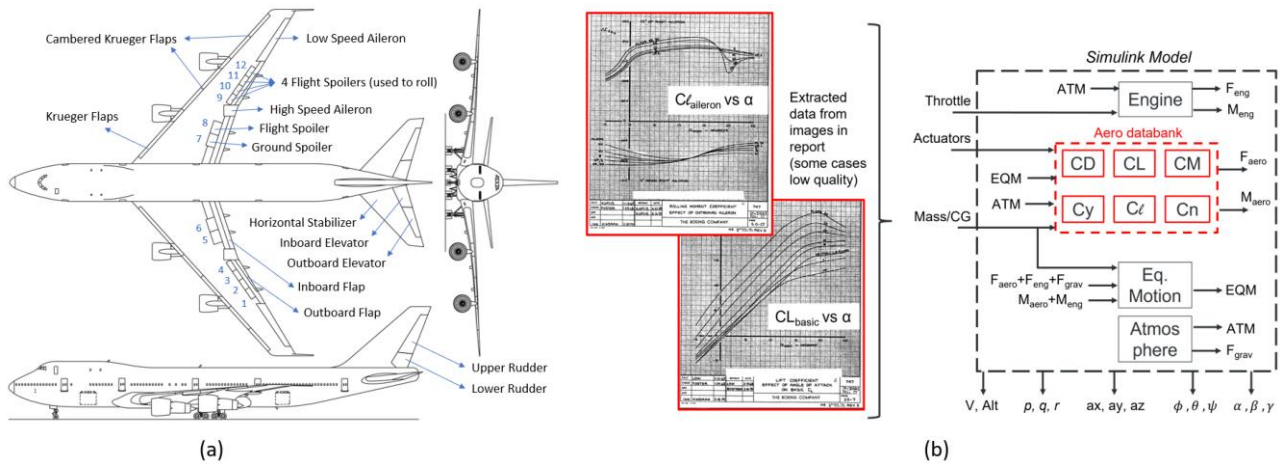


Figure 1 – (a) Views of Boeing 747-100. (b) Data extracted from report NASA (1970) to build aerodynamic model.

## LATERAL-DIRECTIONAL CONTROL LAWS

In the context of aircraft lateral control (rolling axis), it is common to employ roll spoilers together with ailerons, working in collaborative way, in order to achieve requirements that ailerons only are not able to comply (low control power in some points of flight envelope for example). This is usually referred to as lateral control allocation. The challenge of control allocation in this context is to compute deflections of aileron and roll spoiler that comply with requirements of stability, performance, and handling qualities. Two approaches of control laws are proposed and adopted for case study in the context of PIO due to rate limiting (Category II).

### Method 1: Aileron + Roll spoiler with dead zone

One possible approach, called *Method 1* in this work, is to deflect only ailerons for small roll commands (cases of small corrections), but deflect ailerons together with spoilers in case of large roll commands (cases which require more agility). Moreover, in linear design, for sake of simplification, it is adopted a unique entity for lateral command (*Artificial Aileron*), which will be converted into actual deflections for aileron and roll spoilers during nonlinear design phase (Figure 2(a)). The benefits of this approach are:

- 1) to avoid deflection of spoiler when it is not necessary;
- 2) simplify the roll control surface, by reducing the number of states for optimization of LQR (linear-quadratic regulator) during control gains computation.

However, the limitations of Method 1 are:

- 1) since deflections of aileron and roll spoiler are related (same set of controller gains), there is limited flexibility to adjust separately the deflections of aileron and roll spoiler;
- 2) when aileron is deflecting alone in the range of spoiler dead zone there is a risk for aileron rate saturation, which a known contributor factor for Pilot-Induced Oscillations (PIO).

### Method 2: Aileron + Roll spoiler without dead zone

Another possible approach, called *Method 2* in this work, assumes the availability of a reliable aircraft model for design, specially capturing the nonlinearities of spoiler around neutral positions. With this approach, ailerons and roll spoilers deflect whenever there is lateral command. Roll spoiler can be tuned to provide initial moment with agility and reduce deflection in steady state. Following this approach, aileron and roll spoilers are designed separately. The benefits of this approach are:

- 1) roll spoilers always alleviate the workload of ailerons (reducing risk of rate saturation);
- 2) there is significant flexibility to adjust separately the deflections of aileron and roll spoiler tuning separately the gains of each control surface.

However, the limitations of Method 2 are:

- 1) there are more gains for control design. Using LQR approach, it is necessary to prioritize certain states for optimization and convergence;

2) it is assumed that the airframe model has a good representation of system dynamics.

Figure 2 illustrates the process to convert *Artificial Aileron* deflections into actual Aileron and Roll Spoiler deflections. Note the dead zone of roll spoiler gearing (Figure 2(a)) and the steeper inclination of Aileron gearing to compensate the roll command in the range that aileron works alone.

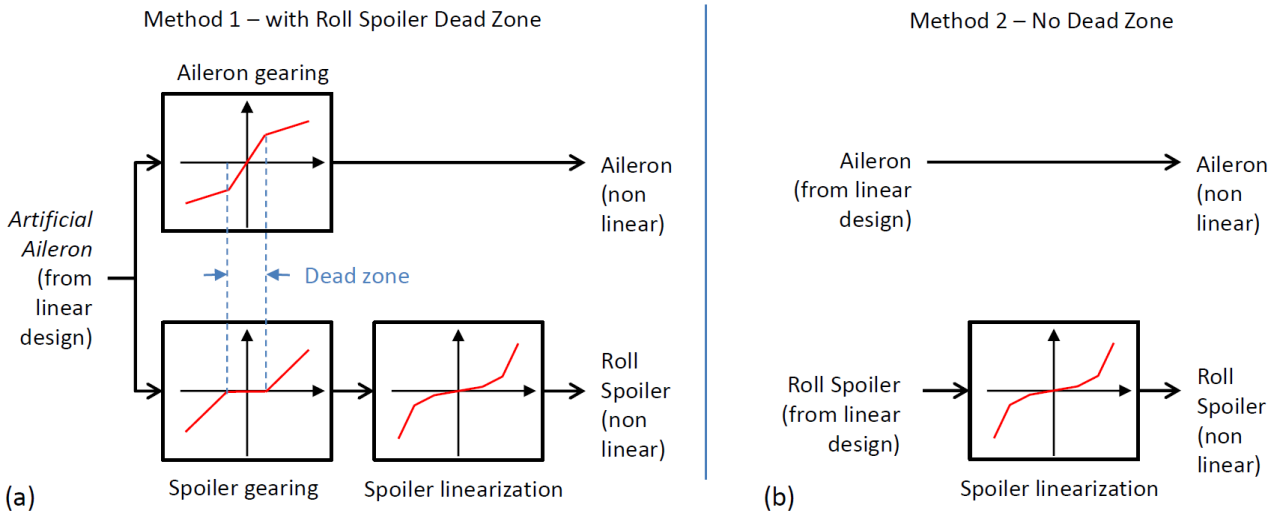


Figure 2 - Simplified strategies for control allocation involving aileron and roll spoilers.

**Control objectives**

This work adopted as case study two versions of regulators for  $\phi'$  (Euler roll angle rate) and  $\beta$  (sideslip angle), using different methods of control allocation for aileron and roll spoilers. The selection of the regulated variables  $\phi'$  and  $\beta$  is a natural one, since these are the variables that either a pilot or an autopilot shall control in order to achieve the desired trajectory path in terms of lateral-directional dynamics. The control architectures analyzed in this study are adaptations of usual controllers referred to in literature as “p-beta” (controllers for roll rate and angle of sideslip), such as presented in the references Berger et al. (2013), Gripp (2015). Related longitudinal control laws for same aircraft are described in the reference Moreira et al. (2022).

**PRACTICAL RESULTS OF OLOP CRITERION USING LINEAR MODELS**

This section illustrates the practical determination of OLOP, following guidelines from Duda (1997). A linear model of the aircraft including the Flight Control System (FCS), the location of the relevant rate limiter, and information about maximum stick deflections (e.g., maximum command authority) and maximum rates must be available. To facilitate the determination of relevant frequency responses in certain portion of Pilot-Vehicle System, Figure 3 highlights the inputs and outputs adopted in each step of OLOP criterion. Figure 3(a) shows the closed loop involving models for “Pilot Model”, “FCS”, “Actuators” (ailerons, roll spoilers, rudder), “Rate limiter”, “Aircraft”, as well as feedback variables for “p-beta” such as  $\phi$  (roll angle),  $r$  (yaw rate),  $p$  (roll rate),  $N_y$  (lateral acceleration),  $\beta$  (sideslip angle). It is important to note that OLOP criterion is adequate to evaluate one rate limiter at a time.

**Simplified closed loop model (rate limiter in 1 actuator)**

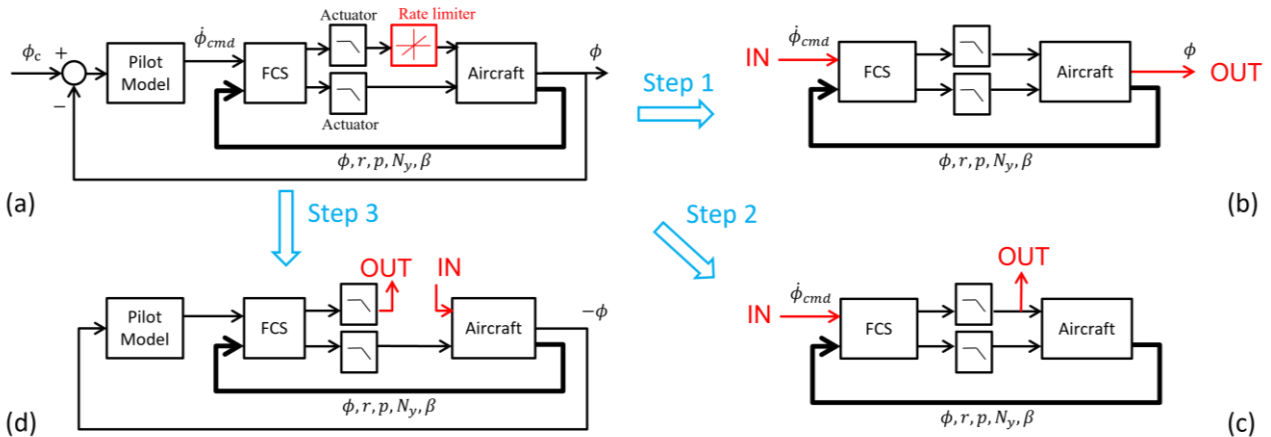


Figure 3 - Steps for OLOP Criterion. (a) Representation of Pilot-Vehicle System (Rate limiter highlighted), (b) Model adopted in Step 1, (c) Model adopted in Step 2, (d) Model adopted in Step 3. Adapted from Duda (1997).

Consider for example trimmed linear models for Aircraft in the following condition: straight and level flight, Flaps 30 deg (fully extended), Weight 350,000 lb (mean value), CG 33% MAC (mean value), 100 KCAS (low speed and control power), Pressure Altitude 3,000 ft, Landing gear up. Same approach can be repeated for other flight conditions. The procedure for the evaluation of the OLOP criterion is summarized in the following three steps.

**Step 1: Define a simple (high) gain pilot model**

“Pilot Model” in Figure 3 can be assumed as a simple gain, since it has a synchronous precognitive behavior during a fully developed PIO, McRuer (1995). This pilot gain can be adjusted based on the linear crossover phase angle of the open-loop aircraft pilot system (Figure 3(b)). Crossovers between -110 to -160 deg (equivalent to linear phase margins of 70 to 20 deg respectively) for the roll axis should be investigated to cover a wide range of possible pilot gains.

Figure 4 presents Nichols plots for closed-loop transfer function from  $\phi'_{cmd}$  (roll angle rate command of pilot stick) to  $\phi$  (roll angle), obtained with a model such as illustrated in Figure 3(b) (rate limiter removed). Multiplicative pilot gains ( $K_p$ ) are applied to original transfer function  $\phi'_{cmd}$  to  $\phi$  (solid red line in Figure 4) in order to identify the pilot compensation which results phase margins of 70 to 20 deg. Additional intermediate case (crossover -135 deg or phase margin equal to 45 deg) is considered. In this example,  $K_p$  equal to 0.32, 2.3 and 13 are obtained for Method 1, whereas  $K_p$  equal to 0.47, 1.7 and 3.5 are obtained for Method 2. The wide range of pilot gains calls attention on this criterion.

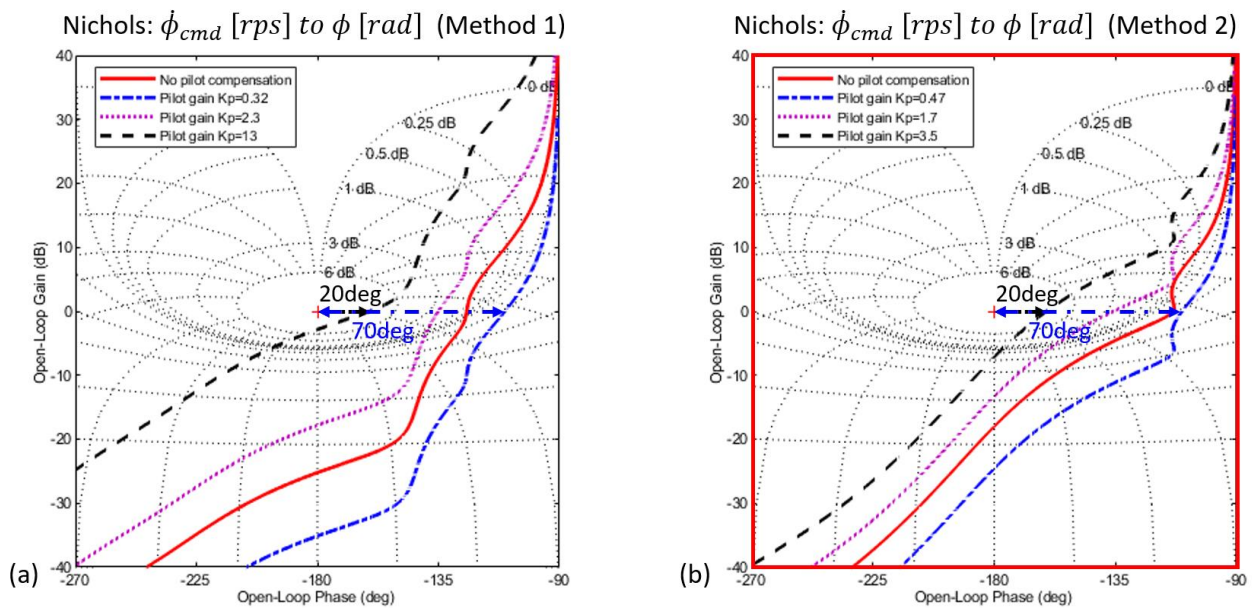


**Figure 4 - Pilot gain compensations ( $K_p$ ) for transfer function  $\phi'_{cmd}$  to  $\phi$  (Figure 3 (b)). (a) Method 1, (b) Method 2.**

**Step 2: Determine the linear closed-loop onset frequency**

Onset frequency ( $\omega_{onset}$ ) is the frequency at which actuator saturation occurs for the first time. It can be determined as the graphical cross of frequency response from stick command to the input of the rate limiter (actuator output in this example) and a straight line with slope -20 dB/decade that crosses 0 dB at the rate limit  $R$ .

Figure 5 presents Bode plots for closed-loop transfer function from  $\phi'_{cmd}$  to actuator model output (input of rate limiter), obtained such as illustrated in Figure 3(c). Maximum rate limits of aileron and roll spoilers for the aircraft under study are  $R=100$  deg/s for total aileron (right minus left hand) and  $R=75$  deg/s for roll spoiler. Three percentages of command authority are considered (50%, 75% and 100%) in order to evaluate  $\omega_{onset}$ , when pilot applies different levels of command.

In this example, *Artificial Aileron* with  $R=100$  deg/s in Method 1 gives  $\omega_{onset} = 1.35$  rad/s if pilot uses 100% of roll rate command (15 deg/s),  $\omega_{onset} = 1.65$  rad/s if pilot uses 75% of roll rate command (11.25 deg/s) and  $\omega_{onset} = 2.21$  rad/s if pilot uses roll rate 50% of command (7.5 deg/s). As expected, the larger the amplitude of pilot command, the lower the onset frequency ( $\omega_{onset}$ ) related to rate limiting, i.e., rate limiting occurs “earlier”. These results indicate that rate limiting in *Aileron Total* might happen at frequency  $\omega_{onset} = 1.35$  rad/s if pilot applies full command, using Method 1 control law. However, for Method 2, the chance of rate limiting in aileron is much lower (necessary high frequency of  $\omega_{onset} = 7.21$  rad/s and full command, which is out of aircraft and pilot bandwidth). Additionally, for Method 2, rate limiting in roll spoiler might happen, but it requires for example  $\omega_{onset} = 2.14$  rad/s and full command. It indicates that spoiler can achieve rate saturation “earlier” than aileron in Method 2, although the frequencies to achieve such scenario are at the boundary of this aircraft bandwidth.

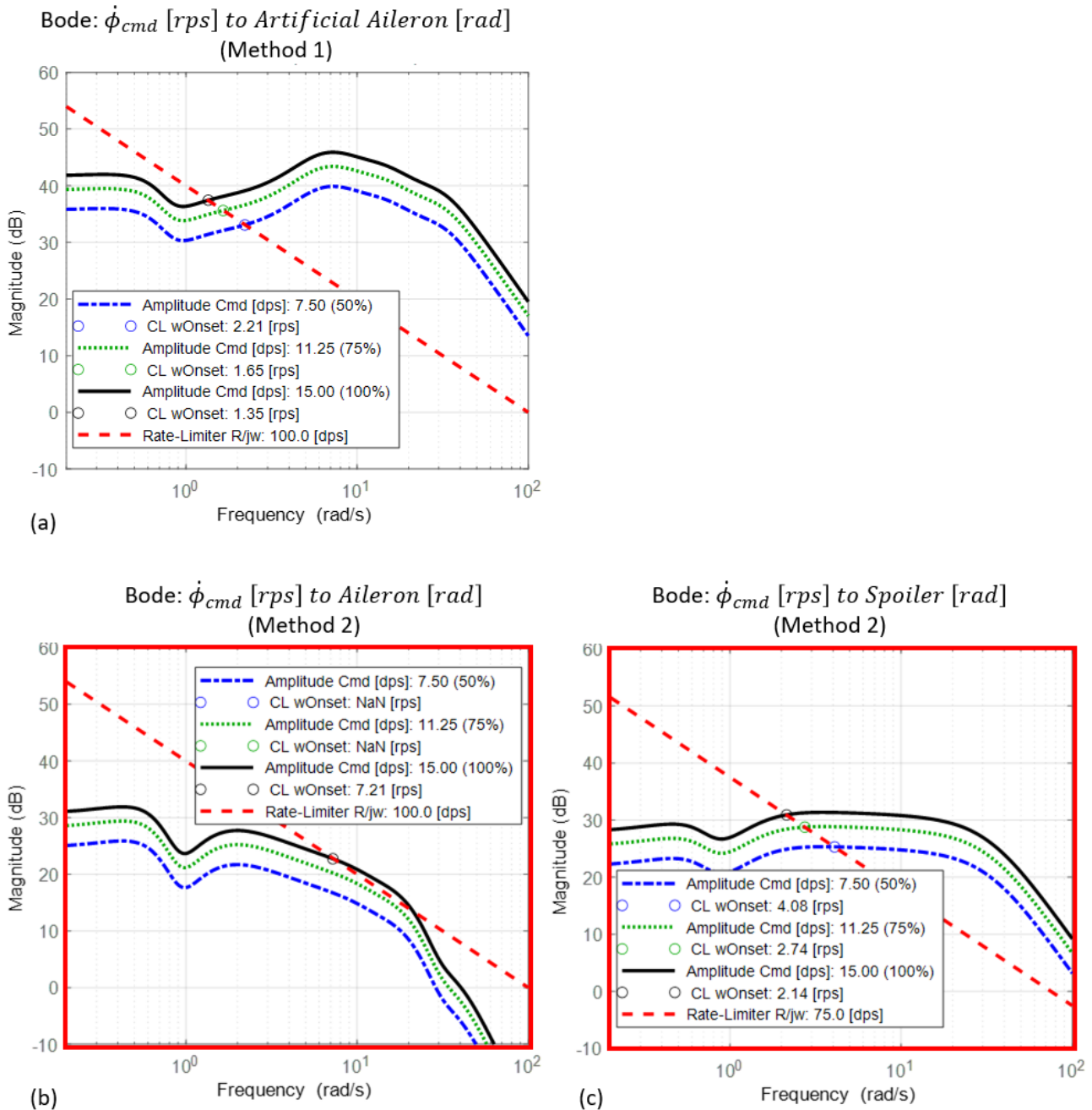


**Figure 5 -  $\omega_{onset}$  determination (Figure 3 (c)), considering different percentages of pilot command. (a) Method 1 (Artificial Aileron), (b) Method 2 (Aileron), (c) Method 2 (Spoiler).**

**Step 3: Compute the open-loop response with loop broken at rate limiter and plot  $\omega_{onset}$  in Nichols chart**

Figure 6 shows the curves of open-loop broken at each rate limiter (Figure 3(d)), considering different pilot gains ( $K_p$ ) in the loop (obtained in step 1). The circles over each curve represent the open-loop onset frequencies ( $\omega_{onset}$ ) obtained in step 2. This analysis is presented for *Artificial Aileron* of Method 1, and separately for aileron and spoiler of Method 2 (highlighted in red). Black dashed line is the boundary proposed by Duda (1997). Cases of  $\omega_{onset}$  above black dashed line indicate PIO prone cases according to OLOP criterion.

In this example OLOP criterion indicates that there is high probability of Category II PIO for Method 1 (Figure 6(a)) if pilot applies more than 50% of command, because all the circles are above the boundary (black dashed line), no matter the range of pilot gain. However, as presented in Figure 6(b) for Method 2, rate limiting in aileron is very unlikely (necessary 100% of command at frequencies above 7.21 rad/s, which is out of aircraft and pilot bandwidth). By the end, according to Figure 6(c), rate limiting in spoiler is unlikely as well, crossing the boundary only if a high-gain pilot ( $K_p=3.5$ ) applies 100% of command in frequencies such as  $\omega_{onset} = 2.14$  rad/s (very specific case).

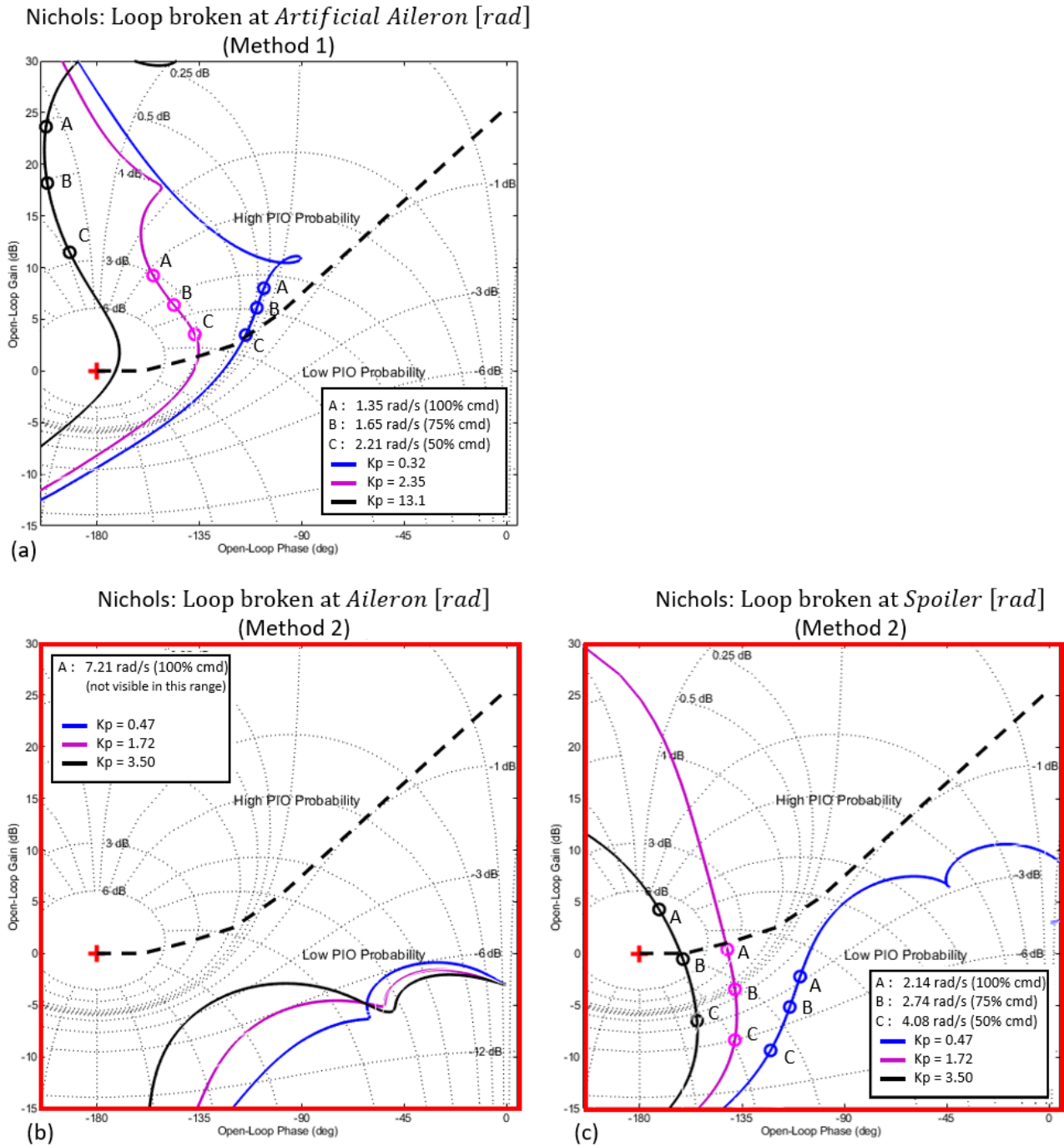


Figure 6 - Nichols charts for loop broken in each rate limiter (Figure 3 (d)). Dashed black line represents the OLOP criterion boundary. (a) Method 1 (Artificial Aileron), (b) Method 2 (Aileron), (c) Method 2 (Spoiler).

### PRACTICAL RESULTS OF OLOP CRITERION USING NONLINEAR MODELS

To check the predictions of OLOP criterion using linear models (previous section), some simulations were performed using a complete nonlinear integrated model containing modeling for aerodynamics databank (section “Aircraft Model”), two methods of control laws (Methods 1 and 2), engines, actuators, sensors, standard atmosphere, traditional 6-degree of freedom equations of motion (integrated model for nonlinear simulation was documented in Gripp et al. (2023)). For comparison, this nonlinear model was initialized in the same trim condition adopted as example in previous section (Flaps = 30 deg; Weight = 350,000 lb; CG = 33% MAC; Airspeed = 100 KCAS; Pressure Altitude = 3,000 ft; Landing Gear up), but similar comparisons can be repeated in other flight conditions. The results of nonlinear simulations are presented in Figure 7.

A forced roll angle command ( $\phi_c$ , such as illustrated in Figure 3(a)) is applied as reference for nonlinear simulation. It has a sinusoidal shape, with frequency equal to  $\omega_{onset}$ . The amplitude ramps in from zero to certain selected amplitude over the first five seconds, followed by thirty seconds of oscillations in same amplitude. The signal ramps out over five seconds at the end of the run. The pilot command for “p-beta” is given by  $\phi'_{cmd} = K_p(\phi_c - \phi)$ .

For “p-beta” with Method 1, consider for example the combination defined by point A of magenta curve in Figure 6(a):  $K_p = 2.35$  (“average” pilot gain) and  $\omega_{onset} = 1.35$  rad/s (assumption that pilot applies 100% of command, i.e.,  $\phi'_{cmd} = 15$ deg/s in this case). By setting empirically the amplitude of reference  $\phi_c$  to 5 deg in order to match the case, it is possible to check that each aileron starts to achieve the maximum values of rate limiting (50 deg/s) when working alone in the range of spoiler dead zone, as illustrated in Figure 7(g). It is justified because in the range of spoiler dead zone, *Artificial Aileron* is purely aileron (Figure 2(a)). This scenario can be thought as a pure-gain pilot ( $K_p=2.35$ ) fine-tracking a sinusoidal reference  $\phi_c$  (plotted for example on a Primary Flight Display), which has 5 deg of amplitude and 1.35 rad/s of frequency. As consequence the pilot would apply full stick in some moments, and aileron would reach maximum rate limiting for short periods (when working without spoiler).

For sake of comparison with Method 2, same input  $\phi_c$  is applied in nonlinear simulation. However, for Method 2 with  $K_p = 2.35$  and  $\omega_{onset} = 1.35$  rad/s the resultant peaks of  $\phi'_{cmd}$  are 10 deg/s (75% of command), as presented in Figure 7(b). Since there is no roll spoiler dead zone for Method 2, aileron and spoiler work together all the time, thus it is necessary less  $\phi'_{cmd}$  to track the same reference  $\phi_c$ . As consequence the rates of aileron are lower when compared to Method 1 (Figure 7(g)). Comparing the results of Method 2 obtained from nonlinear simulation (Figure 7) with OLOP predictions (Figure 6(b)/(c)), the results are compatible for the analyzed scenario, i.e., low risk of rate saturation in aileron and roll spoilers.

Finally, the predictions of OLOP criterion following the steps from previous section can be confirmed with integrated nonlinear model simulations, by setting the same condition. However, the magnitudes of reference  $\phi_c$  must be empirically defined to match the whole scenario. Moreover, there is no guideline about feasible range of frequencies, pilot gains and amplitudes to select. Many combinations from OLOP predictions (some cases might be not feasible) can be compared to nonlinear model. The decision of feasible combinations considering aircraft and pilot limitations is responsibility of designer.

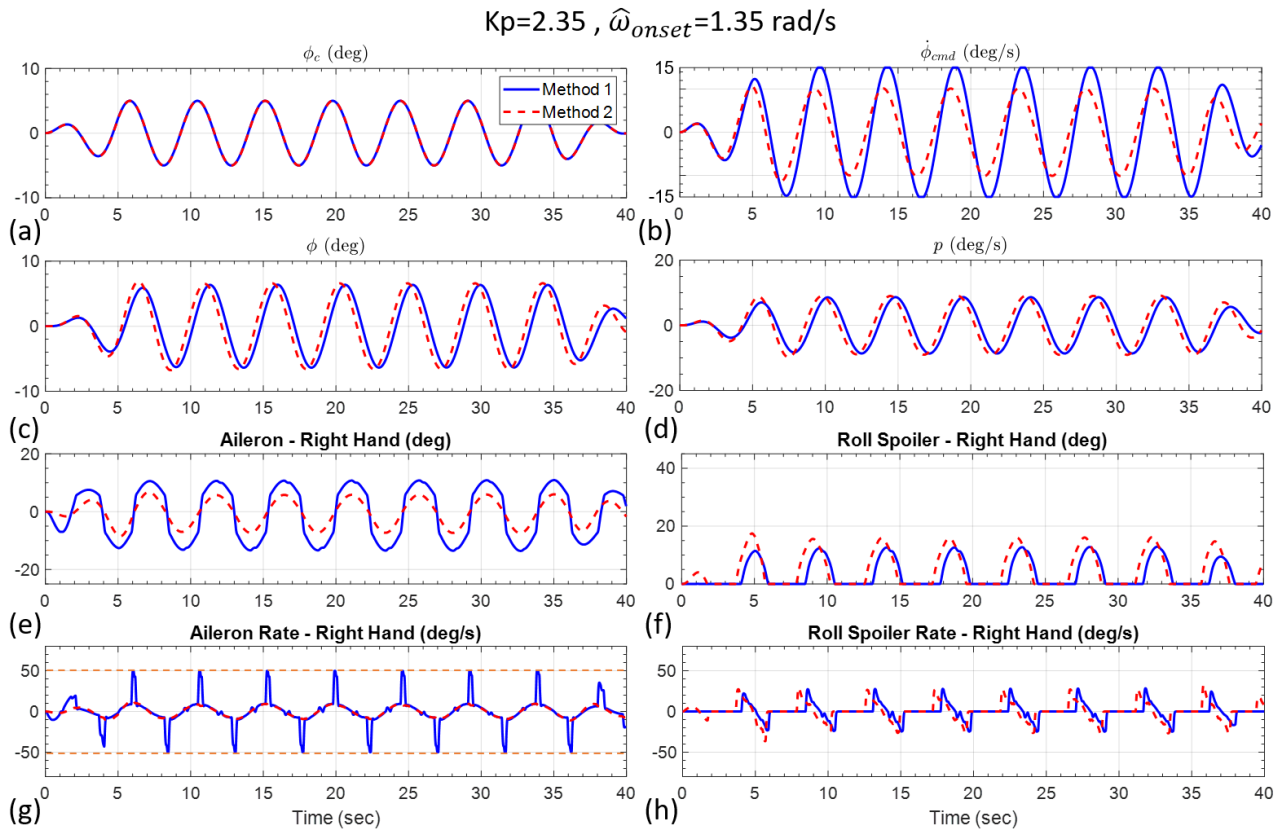


**Figure 7 - Results of nonlinear simulation for sinusoidal reference  $\phi_c$  (amplitude 5 deg, frequency 1.35rad/s) tracked by pilot model  $K_p=2.35$  (structure of Figure 3(a)). It confirms predictions of OLOP criterion in Figure 6.**

## CONCLUSIONS

This paper has investigated the OLOP criterion for predictions of Category II PIO (due to rate limiting) and its practical applicability to real industrial designs of control laws for fly-by-wire aircraft. For case study, it was adopted a large transport aircraft and two versions of lateral-directional control laws. The conclusions are highlighted in the sequence.

As benefit, OLOP criterion gives direction about PIO prone cases: 1) it helps to filter cases in a vast range of flight conditions; 2) it was possible to anticipate by using the OLOP criterion that one version of control law (Method 1 in this

work) is more prone to PIO than other (Method 2 in this work); 3) it is possible to double check the predictions of OLOP criterion against simulations in nonlinear integrated model (points above and below template boundary).

As limitation, OLOP criterion has the following weaknesses: 1) Real pilot gains are not known in advance to apply the OLOP criterion. It motivates try-and-error iterations to identify adequate amplitudes of  $\phi_c$  to be used in nonlinear simulations in order to match the conclusions of OLOP criterion. Moreover, this iterative aspect to find the correct setup for OLOP criterion creates extra difficulties to run the criterion in the whole flight envelope; 2) The proposed range of pilot pure gains seems to be excessive; 3) OLOP criterion does not cover the duration of rate saturation, only the occurrence; 4) OLOP criterion does not distinguish cases in frequency that are not feasible (excessive values beyond pilot or aircraft bandwidth), so it must be filtered by designer.

Based on previous comments, it is possible to conclude that the original OLOP criterion has some limitations to be applied directly as design tool in real industrial control laws designs. It is recommended to use the OLOP criterion as a preliminary step to filter cases in the flight envelope, and additionally to filter again the cases with long periods of rate saturation.

## **ACKNOWLEDGMENTS**

Special thanks to EMBRAER company and ITA (Instituto Tecnológico de Aeronáutica) for providing infrastructure, tools, and personnel (pilots and engineers) which contributed with the development of this work.

## **REFERENCES**

- Klyde, D. H., McRuer, D. T., Myers, T. T., “Unified Pilot-Induced Oscillation Theory, Vol. I: PIO Analysis with Linear and Nonlinear Effective Vehicle Characteristics, Including Rate Limiting”, Wright Lab., WL-TR-96-3028, 1995.
- Nguyen, D. H., Lowenberg, M. H., Neild, S. A., “Effect of Actuator Saturation on Pilot-Induced Oscillation: A Nonlinear Bifurcation Analysis”, *Journal of Guidance, Control and Dynamics*, Vol. 44, No. 5, 2021, pp. 1018–1026.
- Efremov, A., Efremov, E., and Tiaglik, M., “Advancements in Predictions of Flying Qualities, Pilot-Induced Oscillation Tendencies, and Flight Safety”, *Journal of Guidance, Control and Dynamics*, Vol. 43, No. 1, 2020, pp. 4–14.
- USAF. “Military standard - Flying qualities of piloted aircraft”, MIL-STD-1797B, 2006.
- GARTEUR. “Evaluation of Prominent PIO Susceptibility Criteria”, TP-120-01, 1999.
- Duda, H., “Prediction of Pilot-in-the-Loop Oscillations Due to Rate Saturation”, *Journal of Guidance, Control and Dynamics*, Vol. 20, No. 3, 1997, pp. 581–587.
- NASA, “The Simulation of a Jumbo Jet Transport Aircraft Volume II: Modeling Data”, NASA D6-30643, USA, 1970.
- Gripp, J. A. B., Moreira, M. A. G., Trabasso, L. G., Marinho, C. M. P. “Configuration of aerodynamics model in flight simulator to investigate Pilot-Induced Oscillations and Loss of Control”, *Proceedings to the XIX International Symposium on Dynamic Problems of Mechanics (DINAME)*, ABCM, 2023.
- Berger, T., Tischler, M. B., Hagerott, S. G., Gangsaas, D., and Saeed, N., “Lateral/directional control law design and handling qualities optimization for a business jet flight control system”, *AIAA Atm. Flight Mec. Conference*, 2013.
- Gripp, J. A. B., “Lateral and Directional Control Law Design for Business Jet Employing LQR with Adjust of Transmission Zeros and Gain Scheduling Techniques”. *Masters of Science (ITA)*, Brazil, 2015.
- Moreira, M. A. G., Gripp, J. A. B., Yoneyama, T., and Marinho, C. M. P., “Longitudinal Flight Control Law Design with Integrated Envelope Protection”, *Journal of Guidance, Control and Dynamics*, 2022, pp. 1–11.
- McRuer, D. T., *Pilot-Induced Oscillations and Human Dynamic Behavior*, NASA, USA, 1995, pp. 1–86. NASA4683.

## **RESPONSIBILITY NOTICE**

The authors are the only responsible for the printed material included in this paper.